NUMERICAL SIMULATION OF FLUID FLOW AND HEAT TRANSFER AROUND TURBINE BLADES

Shashidhara B J[1], Arunkumar G L[2]

[1]M.Tech, Dept. of TPE, NMIT Bengaluru, [2]Professor, Dept of TPE NMIT Bengaluru,
Email:srgowda03@@gmail.com

--***---

Abstract - *A turbine is a machine having minimum one moving part called a rotor gathering, which is a pole with sharp edges connected. The principle point of the paper is to check the part of warmth exchange on the sharp edges by making the openings on it. To make this the examination is made for aerofoil with holes, without openings considering with and without temperature and a similar thing is made for turbine. From the weight shape chart, the variety of speed stream over the turbine is seen. As the speed builds step by step and afterward diminishes in the trailing edge. The variety of speed stream over the turbine is seen from the speed vectors. At driving edge of the turbine and in the camber part distribution impact is unmistakably appeared for both with gaps and without openings. Torque strengths are diminished and temperature is diminished for turbine with openings because of the warmth exchange rate. Furthermore, the examination is finished with all turbulence models.*

Key Words: turbine, blades, temperature, pressure, flow, velocity…

1. INTRODUCTION

M. Papa et.al [1] studied the effect of secondary flows on mass transfer from a gas turbine blade and hub wall measurement using a method called naphthalene sublimation by providing the non dimensional mass transfer in the form of Sherwood numbers, that can be converted to heat transfer coefficients by using suitable analogy, Yao Yu et.al[2] did the investigation on the numerical research on the film cooling performance of a single row of converting slot holes on the blade suction side in an engine in which the Reynolds number is from $4*10^5$ to $6*10^5$ and blowing ratio is varied between 0.5 to3. A comparison to a cylindrical hole was made and effect of major factors on the film cooling effectiveness and aerodynamic loss were explored, including the film hole location ratio and primary flow Reynolds number.

Sang Woo Lee et.al [3] studied the aerodynamic performance of a turbine cascade with 2 different types of winglet covering the tip gap inlet of a plane tip, one is pressure side (PS) winglet and another one is leading edge pressure side (LEPS) winglet, for a tip gap height to chord ratio 2%, their width to pitch ratio 2.64%, 5.28% and 10.55%. The experimental outcome shows that ps winglet reduces aerodynamic loss in the tip leakage vortex region as well as

in the area downstream of the winglet pressure surface corner, where as it increases aerodynamic loss in the central area of the passage vortex region. Heeyoon Chung et.al [4] did an experiment on improved array to enhance the cooling performance of a perforated blockage. Here the internal passage in the trialing region of the blade was modeled as a wide square channel with 3parellel blockages. Various types of perforated blockage were tested with a fixed Reynolds number based on the channel hydraulic diameter. In the lateral direction baseline design had holes positioned along the centerline of the blockage. The hole size, array pattern, hole direction were altered to enhance the cooling performance.

2. MODELING

The turbine sections are based on the modification to the customized NACA 6 and 7 series aerofoil. The blade extrusion problem is handled by modifying the blade geometry near the hub so that the blade emerged from it is nearly perpendicular. The blade sections resemble aerofoil: the values are taken from the blade section geometry. Using CATIA V5 these generated profiles are surfaced and exported to the STARCCM+ solver.

2.1 Design And Model Geometry

Initially the coordinates which was in .txt format was converted into CATIA V5 acceptable format that is .ascii. The created .ascii format coordinates was imported into CATIA V5 and using spline operation the coordinates are joined and was padded to 50mm using pad operation as shown in the fig 2.2. In this created aerofoil two holes of 5mm are made at the edges and one hole of 10mm at the center of the aerofoil as shown in fig 2.3. The aerofoils were join to a shaft of diameter 100mm with glue operation and complete cascade with 20 numbers of blades were made using crown operation. Previously designed aerofoil with holes is imported to CATIA and is joined with shaft using glue operation and the complete cascade consisting of 20 blades is created using crown operation.
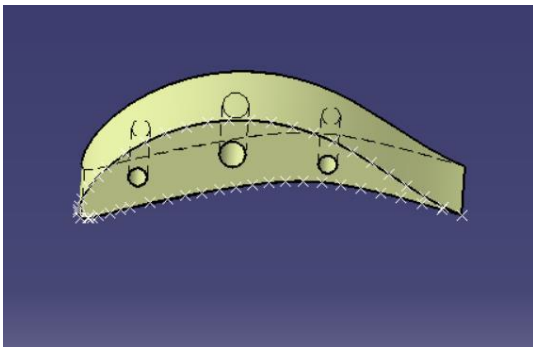

Fig 2.1- shows the aerofoil with 3 holes

Using the glue operation the aerofoils are joined to a shaft of 100mm diameter and complete the cascade using the crown operation with 20number of blades.
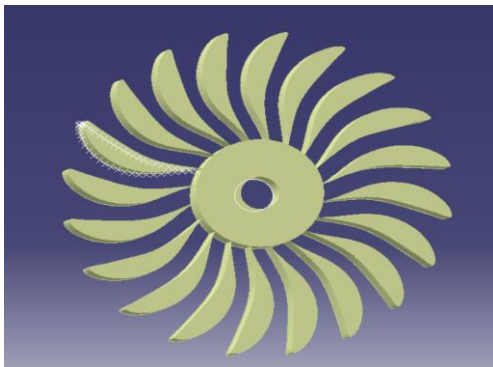

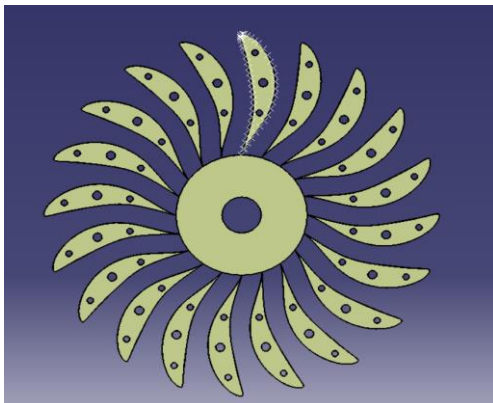**Fig 2.2**- shows the gas turbine cascade without holes

Fig 2.3- shows the gas turbine cascade with holes

These data are splined to generate a surface representation of the whole blade. The hub is an ax symmetric surface specified by a curve which is rotated about the turbine axis. The other blades are easily regenerated by copying and rotating the reference blade for with holes and without holes is shown in Figs. 2.4 and 2.5.

3. MESH GENERATION

Mesh generation is the process of obtaining the appropriate mesh or grid. Specialized software programs have been developed for the use of mesh generation. Generation of polyhedral meshes are easy to execute. When a surface grid has been created, tetrahedral that have one base on the surface are generated above it and the process is continued towards the center of the volume along a marching front. Polyhedral cells are not desirable near walls if the boundary layers needs to be resolved because the first grid point must be very close to the wall while relatively large grid sizes can be used in the directions parallel to wall. Fig 3.1 to 3.2 shows the meshing and sectional views of aerofoil. Meshing over the turbine blades, magnified views and sectional views of turbines with and without holes are shown in Fig from 3.3 to 3.4.
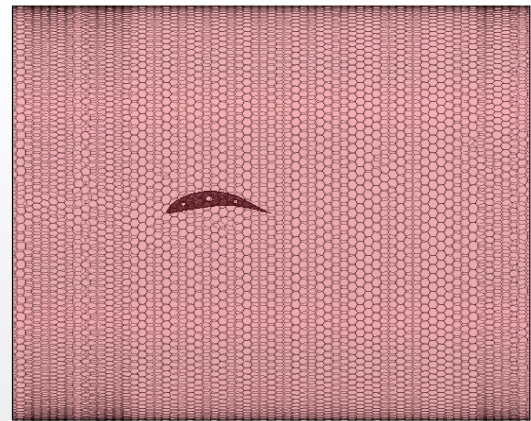

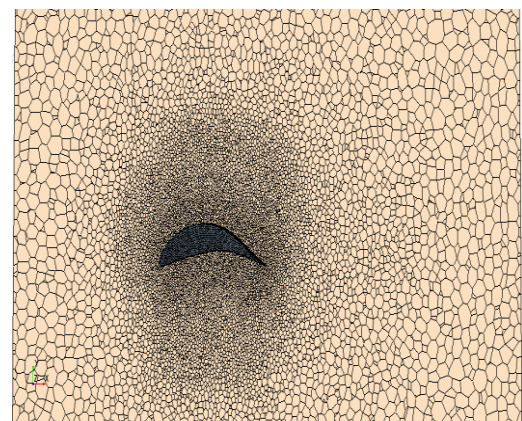**Fig 3.1**- shows polyhedral mesh in computational of aerofoil

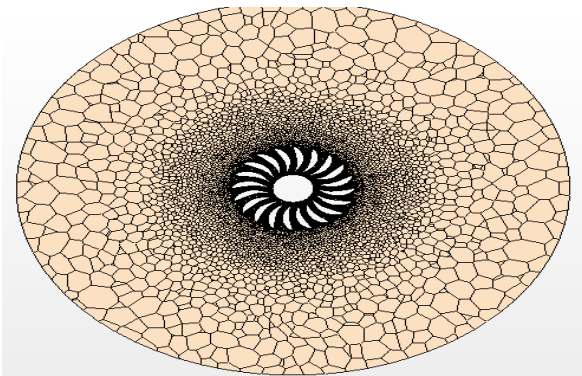**Fig 3.2**-shows aerofoil mesh without holes

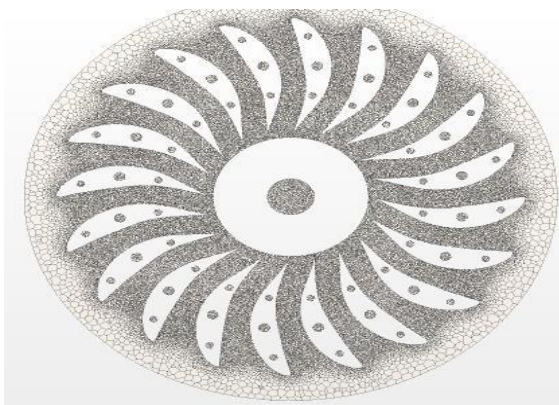**Fig 3.3**- shows the sectional view of turbine

Fig 3.4- magnified view of mesh with holes

4. BOUNDARY CONDITIONS

Boundary conditions are applied to analyse the flow around the rotating propeller in open water. At the inlet velocity component with a uniform speed were imposed. At the outer boundary, the symmetry boundary condition was imposed; on the blade and hub surface, the no-slip condition was imposed. The material properties for water are specified for the domain. The inlet is specified as 'velocity inlet', with the velocity normal to the wall, the velocity and the rate of revolution for various load condition is listed in Table 4.1.

Advance Coefficient (J)	V (m/sec)	N (rps)
0.333	200	3000

Table 4.1 inlet parameters

At the inlet, the turbulence parameters are specified using turbulence intensity of 0.05 Js/kg-m. The outlet face is specified as 'outflow', with reference pressure (atmospheric pressure) value, specified at the outlet face location. The turbulence parameters for various load condition are listed in Table 4.2

Advance Coefficient (J)	OMEGA (in /s)	Local Turbulence Kinetic Energy (k in J/kg)
0.833	0.21	358

5. RESULTS AND DISCUSSIONS

From the Pressure contour diagram, the variation of the velocity of flow over the aerofoil is seen. At the leading edge of the aerofoil, stagnation condition is clearly captured. Also, boundary layer formation is seen near the walls. As the flow advances over the body, the velocity increases gradually and then reduces in the trailing region due to curvilinear nature of the tail geometry with holes and without holes as shown in Figures from 5.1 to 5.2. From the velocity vectors diagram, the variation of the velocity of flow over the aerofoil is seen. At the leading edge of the aerofoil and in the camber part recirculation effect is clearly shown in figures from 5.3 to 5.4 for with holes and without holes. From figures 5.5 to 5.6 Temperature distribution over the aerofoil for with holes and without holes clearly shows the heat transfer rate.
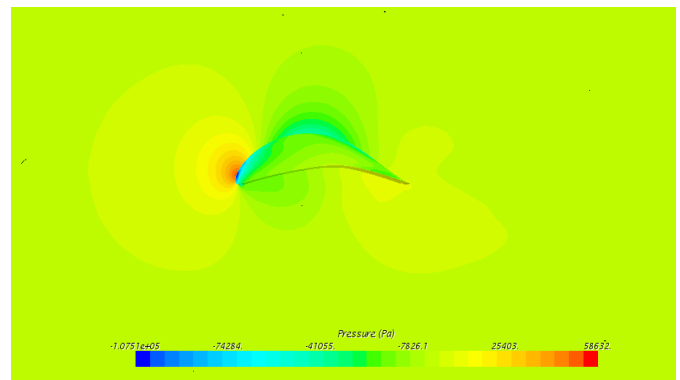

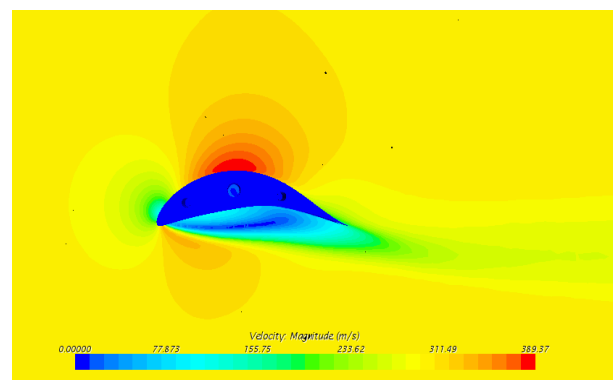**Fig 5.1**- pressure contour on the aerofoil without holes

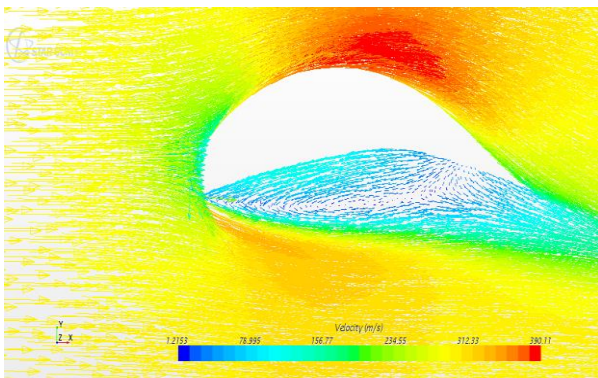**Fig 5.2-** pressure contour on the aerofoil with holes

Fig 5.3- velocity vectors on the aerofoil without holes

Fig 5.4- velocity vectors on the aerofoil with holes

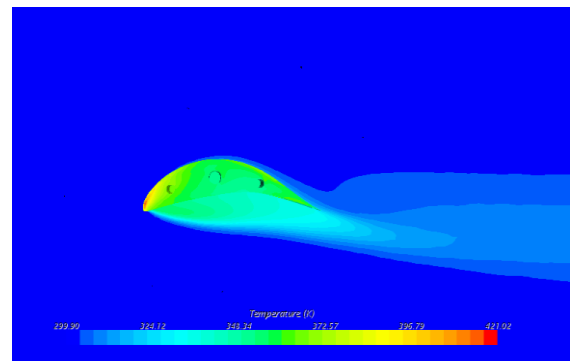**Fig 5.5-** temperature contour on the aerofoil without holes

Fig 5.6- temperature contour on the aerofoil with holes

From the pressure contour diagram, the variation of the velocity of flow over the turbine is seen. At the leading edge of the turbine, stagnation condition is clearly captured. Also, boundary layer formation is seen near the walls. As the flow advances over the body, the velocity increases gradually and then reduces in the trailing region due to curvilinear nature of the tail geometry with holes and without holes as shown in Figures from 5.7 to 5.8. From the velocity vectors diagram, the variation of the velocity of flow over the turbine is seen. At the leading edge of the turbine and in the camber part recirculation effect is clearly shown in figures from 5.9 to 5.10 for with holes and without holes. From figures 5.11 to 5.12 Temperature distribution over the turbines for with holes and without holes clearly shows the heat transfer rate in between the blades.
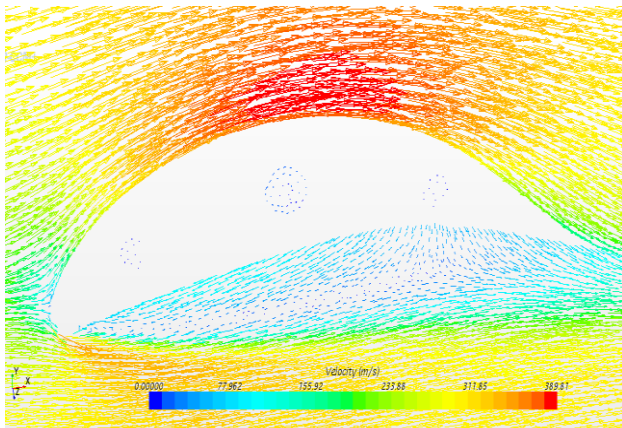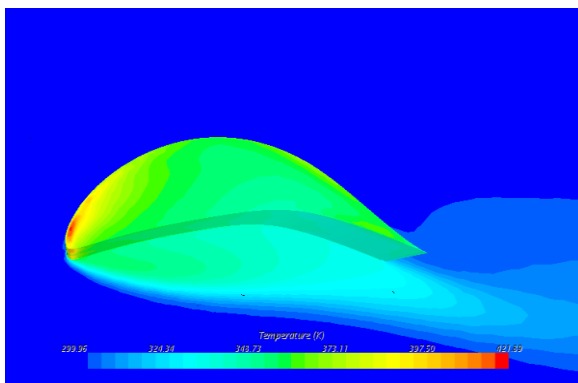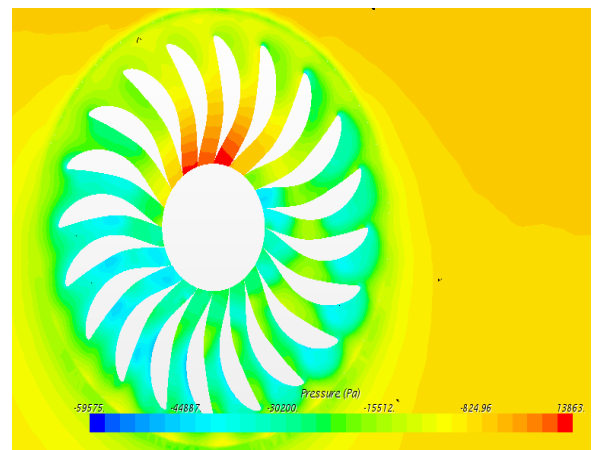

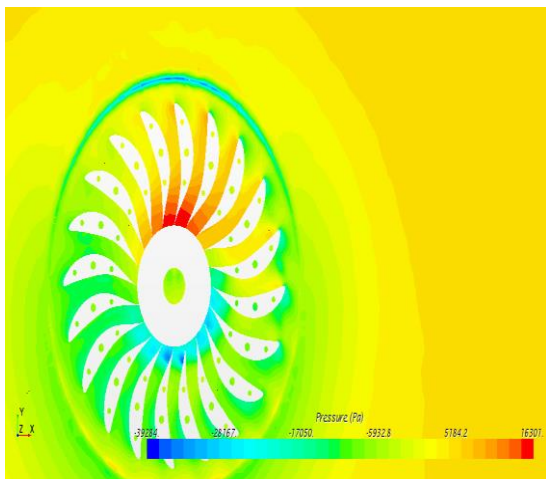**Fig. 5.7-** Pressure contour on the turbine without holes

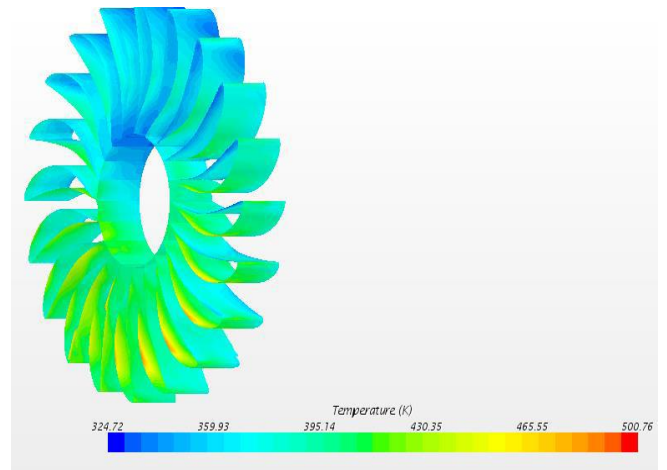**Fig. 5.8-** Pressure contour on the turbine with holes

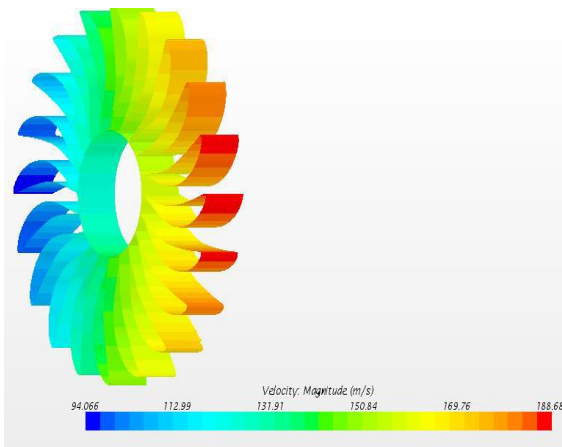**Fig. 5.11**- Temperature contour on the turbine without holes

Fig. 5.9- Velocity contour on the turbine without holes
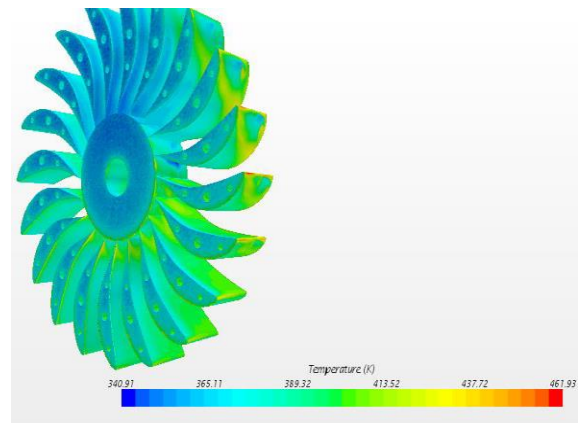
Fig. 5.12- Temperature contour on the turbine with holes

The lift forces, drag force, lift coefficients and drag coefficients for Aerofoil with and without holes in the combination with Temperatures are shown in Table 5.1 and 5.2. By the aerofoil with holes drag and lift forces is increased due to the inner cylinder pushing and pulling forces. The heat transfer rate and torque for turbine with and without holes with Temperatures are shown in Table 5.3 and 5.4. Torque force is reduced and temperature is increased for turbine with holes due to the heat transfer rate.

Fig. 5.10- Velocity contour on the turbine with holes

Table 5.1 Aerofoil With Holes With Temperature

Turbulence models	C_L	C_D	Lift Force {N}	Drag Force {N}
Akn k-epsilon low re	1.467	0.978	74.27	53.16
Eb k-epsilon	1.4636	0.989	74.22	53.23
Realizable K-epsilon	1.4701	0.913	74.23	53.801
Standard K-epsilon	1.4333	0.899	74.89	53.63
Standard K-epsilon low re	1.4697	0.819	74.88	53.27
Standard k-epsilon two layer	1.4001	0.897	74.1	53.17
V2f k-epsilon	1.4982	0.991	74.00	53.812
Realizable k-epsilon two layer	1.4213	0.912	74.69	53.91

Table 5.2 Aerofoil Without Holes With Temperature

Turbulence models	C_L	C_D	Lift Force {N}	Drag Force {N}
Akn k-epsilon low re	1.36	1.03	74.23	52.9
Eb k-epsilon	1.33	1.04	74.22	52.4
Realizable K-epsilon	1.39	1.03	74.21	52.9
Standard K-epsilon	1.42	1.03	74.23	52.3
Standard K-epsilon low re	1.36	1.029	74.23	52.6
Standard k-epsilon two layer	1.39	1.03	74.81	52.6
V2f k-epsilon	1.38	1.04	74.23	52.12
Realizable k-epsilon two layer	1.33	1.03	74.12	52.3

Table 5,3 Turbine With Holes With Temperature

Turbulence models	Torque {N-m}	Heat Transfer {W}
Akn k-epsilon low re	532.77	$1.7996*10^8$
Eb k-epsilon	506.46	$1.7700*10^8$
Realizable K-epsilon	503.25	$1.7719*10^8$
Standard K-epsilon	497.35	$1.7740*10^8$
Standard K-epsilon low re	496.26	$1.770*10^8$
Standard k-epsilon two layer	496.26	$1.7740*10^8$
V2f k-epsilon	508.35	$1.7702*10^8$
Realizable k-epsilon two layer	502.36	$1.7719*10^8$

Table 5.4 Turbine Without Holes With Temperature

Turbulence models	Torque {N-m}	Heat Transfer {W}
Akn k-epsilon low re	532.77	$1.7696*10^8$
Eb k-epsilon	506.46	$1.7700*10^8$
Realizable K-epsilon	502.92	$1.7719*10^8$
Standard K-epsilon	497.35	$1.7740*10^8$
Standard K-epsilon low re	496.56	$1.7750*10^8$
Standard k-epsilon two layer	497.54	$1.7741*10^8$
V2f k-epsilon	508.35	$1.7702*10^8$
Realizable k-epsilon two layer	502.36	$1.7719*10^8$

6. CONCLUSION

The simulations are ran for aerofoil with and without holes with considering Temperatures for eight turbulence models. Simulations are ran for turbine with and without holes in the combination with considering Temperatures for all eight turbulence models. From the Pressure contour diagram, the variation of the velocity of flow over the turbine is seen. At the leading edge of the turbine, stagnation condition is clearly captured. Also, boundary layer formation is seen near the walls. As the flow advances over the body, the velocity increases gradually and then reduces in the trailing region due to curvilinear nature of the tail geometry with holes and without holes. From the velocity contour diagram, the variation of the velocity of flow over the turbine is seen. At the leading edge of the turbine, stagnation condition is clearly captured. Also, boundary layer formation is seen near the walls. As the flow advances over the body, the velocity decreases gradually and then reduces in the trailing region due to curvilinear nature of the tail geometry with holes and without holes. From the velocity vectors diagram, the variation of the velocity of flow over the turbine is seen. At the leading edge of the turbine and in the camber part recirculation effect is clearly shown for with holes and without holes. Temperature distribution over the turbines for with holes and without holes clearly shows the heat transfer rate in between the blades. By the aerofoil with holes drag and lift forces is increased due to the inner cylinder pushing and pulling forces. Torque force is reduced and temperature is decreased for turbine with holes due to the heat transfer rate. Fabrication is made as per the design. Furthermore studies is required for the advancements of the turbine.

REFERENCES

[1].Sang Woo Lee ,Seon Ung Kim, Kyoung Hoon, Aerodynamic performance of winglets covering the tip gap inlet in a turbine cascade International Journal of Heat and Fluid Flow 34 (2012) 36–46

[2] Heeyoon Chung, Jun Su Park, Ho-Seong Sohn, Dong-Ho Rhee, Hyung Hee Cho. Trailing edge cooling of a gas turbine blade with perforated blockages with inclined holes International Journal of Heat and Mass Transfer 73 (2014) 9–20

[3].M. Papa, R.J. Goldstein, F. Gori. Numerical heat transfer predictions and mass/heat transfer measurements in a linear turbine cascade Applied Thermal Engineering 27 (2007) 771–778

[4].Yao Yu , Zhang Jing-zhou, TanXiao-ming, Numerical study of film cooling from converging slot-hole on a gas turbine blade suction side ,International Communications in Heat and Mass Transfer 52 (2014) 61–72

[5].Mohammad H. Albeirutty, Abdullah S. Alghamdi, Yousef S. Najjar., Heat transfer analysis for a multistage gas turbine using different blade-cooling schemes ,Applied Thermal Engineering 24 (2004) 563–577

[6].S. Han, R.J. Goldstein validated the heat/mass transfer analogy from separate heat transfer and mass transfer measurements on simulated turbine blades with equivalent experimental and geometric conditions.